

## Low energy positron interactions – trapping, transport and scattering

J. P. Sullivan<sup>1</sup>, S. J. Buckman<sup>1</sup>, A. Jones<sup>1</sup>, P. Caradonna<sup>1</sup>, C. Makochekanwa<sup>1</sup>, D. Slaughter<sup>1</sup>, Z. Lj. Petrović<sup>2</sup>, A. Banković<sup>2</sup>, S. Dujko<sup>2,3</sup>, J. P. Marler<sup>2,4</sup> and R. D. White<sup>3</sup>

<sup>1</sup> ARC Centre for Antimatter-Matter Studies, Research School of Physical Sciences and Engineering, The Australian National University, Canberra, ACT, Australia

<sup>2</sup> Institute of Physics Belgrade, University of Belgrade, Pregrevica 118, POB 68, 11080 Zemun Serbia

<sup>3</sup> ARC Centre for Antimatter-Matter Studies, School of Mathematics, Physics and IT, James Cook University, Townsville 4810, QLD, Australia

<sup>4</sup> University of Aarhus, Aarhus Denmark

jps107@rsphysse.anu.edu.au

**Abstract.** Recent experiments, theory and modelling of positron interactions with atoms and molecules are discussed. The first half of the paper is devoted to binary collisions between positrons and crossed beams of atoms or molecules (in this case neon) and the second half deals with ensembles of non-interacting positrons, otherwise known as swarms which are transported through the background gas. We review the recent results on measurements of the cross sections based on obtained from collisional positron traps and subsequent calculations of transport properties of positron swarms that may be used to model thermalization experiments, collisional traps and possible applications of positrons in materials science and biomedicine. It was found that kinetic phenomena occur in positron transport that are mainly the result of the positronium (Ps) formation which has a larger cross section than elastic scattering in most gases and at the same time is a non-conservative process. Most importantly negative differential conductivity (NDC) occurs only for the bulk drift velocity while it does not exist for the flux property, a phenomenon that has not been observed for electrons.

### 1. Introduction

Over the past 40 years or so electron scattering data have been obtained experimentally by the application of two techniques. Quasi-monoenergetic beams were employed to obtain the energy dependence of scattering processes, angular differential cross section data and the fine structure and contribution to the cross sections of negative ion resonances [e.g. 1, 2]. However, many of these approaches lacked the ability to produce good quality absolute data and comprehensive data sets that

included all processes. On the other hand, measurements of transport properties of ‘swarms’ of particles in gases (a ‘swarm’ is an ensemble of particles that do not interact with each other, their behaviour being determined by an external electric field and their collisions with the unperturbed background gas) provided data which can be directly applicable in the modelling of low temperature (non-equilibrium) plasmas. These approaches also gave the necessary data to obtain a full set of cross sections for a particular gas through an iterative approach, consisting of solutions to the Boltzmann equation and subsequent modifications of the cross sections in order to reduce the disagreement between the calculated and the measured transport data. The swarm derived cross sections [3, 4, 5] gave good absolute values and total summed balances of number, energy and momentum albeit with a poorer resolution, non-uniqueness and with limits in applicability to lower mean energies (typically below  $\sim 10$  eV). Most importantly the result of the swarm analysis was obtained by averaging over a very broad distribution of particles that is exactly the same as in most non-equilibrium plasmas. Advantages and limitations of the two techniques have been discussed in the past and, if one weighs the pros and cons of both approaches, a joint, complementary approach seems to be the best strategy and this is still valid today. In some cases contemporary beam measurements [6, 1] can match the accuracy of swarm derived cross sections with the flexibility in energy resolution and range, while swarm calculations have become the backbone of the models of collisional plasmas [7]. However there remain, unfortunately, very few joint efforts to produce new cross section data.

In the case of positron interactions with atoms and molecules neither of the two approaches outlined above were easily implemented in the past. This is as a result of significant difficulties in performing positron swarm measurements (see [8]). Positron beam experiments have provided the bulk of the experimental cross section information but these too have been limited in applicability due to low beam fluxes and insufficient energy resolution (see for example [9] and references therein). In this paper we attempt to illustrate how recent advances in beam techniques have enabled a reopening of the positron transport studies, which may eventually benefit those devices that use positrons (e.g. in materials and biomedical research). Here we combine the efforts of both the beam and transport groups from the Australian Centre for Antimatter and Matter Studies with the input of their associated colleagues from Belgrade in an attempt to show the present status of positron scattering and transport studies, and point out the need for future developments and combined efforts.

## **2. Low energy positron scattering from neon**

Since the development of the Surko buffer-gas trap for storing positrons and forming a high resolution, low energy positron beam [10, 11], a number of new and improved experiments have been possible in the field of positron scattering. High resolution beams and new scattering techniques have begun to provide new insight into low energy positron interactions with atoms and molecules [12, 13]. In particular, for the noble gases, it is now possible to perform measurements of scattering with a degree of precision that is far in excess of that previously possible. Improved energy resolution also makes possible the examination of threshold effects and the search for positron scattering resonances, the elusive analogue to negative ion resonances in electron scattering.

In addition, there is now sufficient experimental and theoretical data available to start modelling the transport of positrons on gases, a process that can be expected to proceed in a manner quite different to electron transport – which has been studied for many years. In particular, by modelling the trapping process, it may be possible to gain new insight into the mechanisms that give rise to the effectiveness of buffer gas trapping.

Surko traps are based on a modified Penning-Malmberg trap, with positrons confined axially in a magnetic field of up to 1.5 kG. Confinement in the axial direction is achieved by introducing the positrons to an electrostatic potential well, filled with a mixture of  $N_2$  and  $CF_4$  gases. Positrons lose energy initially by exciting an electronic state of the  $N_2$  (principally the  $a1\Pi$  state) and become trapped in the potential well structure. After becoming trapped, they continue to lose energy through inelastic collisions on the buffer gas, through electronic, vibrational and rotational excitation. In this way, the positrons fall to the bottom of the potential well, and thermalise to the gas temperature, typically room

temperature. This provides a reservoir of positrons with a temperature of approximately 40 meV, which can then be used to form a magnetised positron beam.

The apparatus used for the experiments presented in this paper is based on this technique, and its operation has been described in detail elsewhere [14], only a brief overview will be given here. Positrons from a neon-moderated  $^{22}\text{Na}$  source are directed into an electrode assembly contained in a 500 gauss magnetic field. The electrodes contain a buffer gas mixture of  $\text{N}_2$  and  $\text{CF}_4$ , and positrons exciting electronic transitions in the gas are trapped and subsequently cool to room temperature, as described above. The cooled positrons are emitted from the trap as a pulsed beam, with an energy spread of approximately 60 meV, and are directed to a scattering cell (also in a 500 gauss magnetic field) which contains the target gas. The relative potential of the final stage of the trap and the scattering cell determines the collision energy, which can be tuned from  $\sim 0.5$  to 100 eV. Scattering events redistribute energy in the components of the positron motion parallel and perpendicular to the confining magnetic field. The beam is then directed to a retarding potential analyser to analyse the energy distribution within the beam, before being directed to an microchannel plate assembly for detection. Analysis of the energy distribution gives the cross section values, with normalisation dependent only on the length of the gas cell and the pressure of the target gas inside the cell.

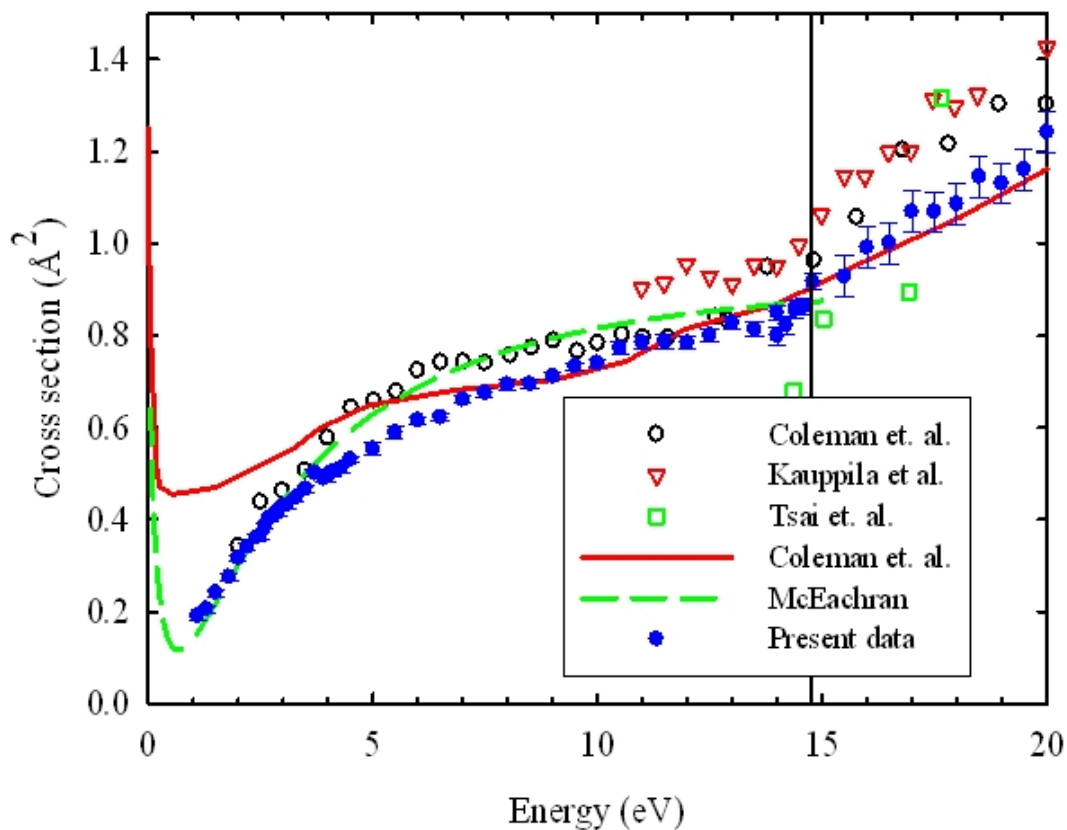


Figure 1: Low energy grand total cross section for positron scattering from neon. Present experiments are the solid circles. Data is compared to previous measurements of Coleman et al. [15], Kauppila et al. [16, 17] and Tsai et al. [18] as well as calculations by Coleman et al. [19] and McEachran [20], as detailed in the legend.

Presented here are preliminary results for positron scattering from neon. The grand total cross section, from 1 to 60 eV has been measured, as has the positronium formation cross section, from threshold to 60 eV. The grand total cross section for the low energy region is shown in Figure 1.

Below the positronium formation threshold, this is equivalent to the elastic scattering cross section. The data is compared with a number of recent theoretical calculations and previous experiments. For the lowest energies, below about 5 eV, the agreement between the recent theory of McEachran [20] and the experimental data is very good, showing the characteristic fall of the cross section associated with the Ramsauer-Townsend minimum. Between 5 eV and the positronium formation threshold, the experiment and theory disagree by up to 10%, well outside the experimental (absolute) error. There is also disagreement in this energy range between the other two experimental measurements, which falls outside the combined errors of the measurements. Conversely, agreement with the theory of Coleman et al. [19] is better at higher energies, above about 8 eV.

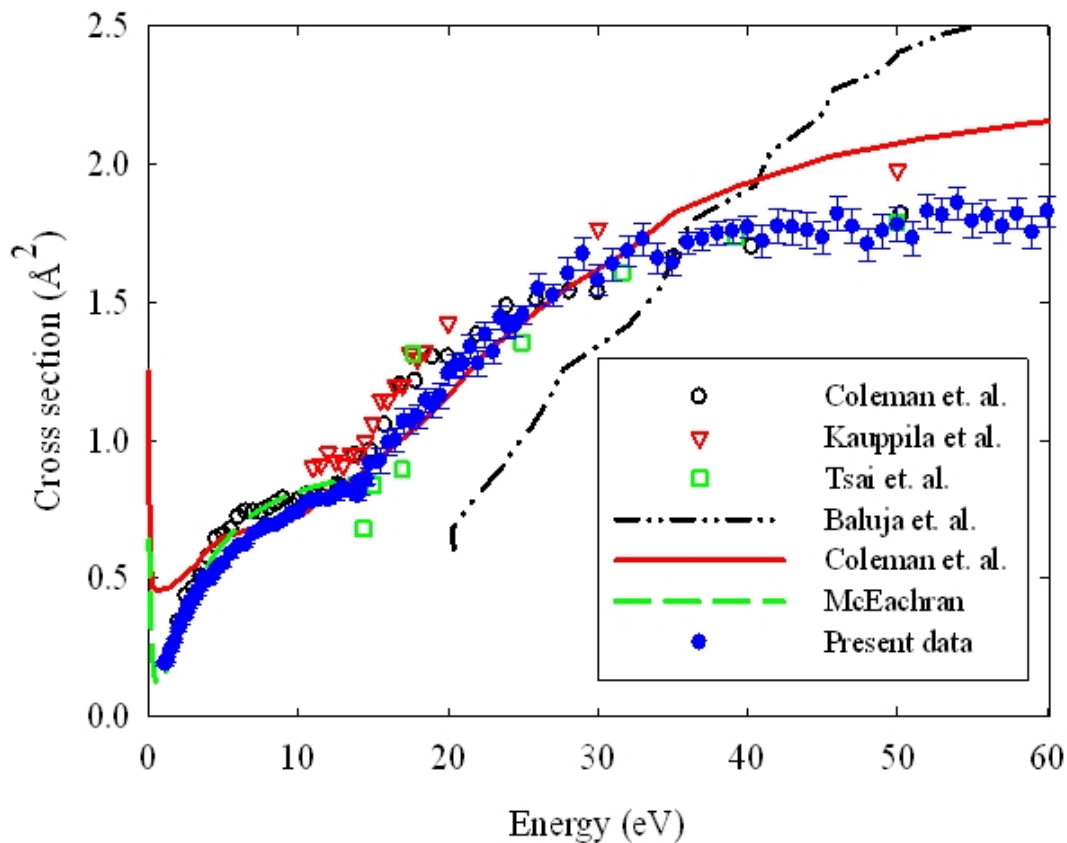


Figure 2: Grand total cross section for positron scattering from neon up to 60 eV incident energy. The data on the plot is as for Figure 1, with the addition of the theory of Baluja et al. [21].

Figure 2 shows the extended energy range measurements. Over this energy range, agreement with previous measurements is generally good, with the exception of the data from the Detroit group [16, 17] which is systematically higher than the present measurements. Agreement with the theory of Coleman falls away from about 30 eV, and the agreement with the calculations of Baluja et al. [21] is quite poor. Generally, while agreement between experiments for the grand total cross section is reasonable, there are still substantial discrepancies that remain and which obviate against claiming these results to represent a ‘benchmark’ standard of cross section. The recent theory of McEachran appears to be a much better description of the scattering system below the Ps threshold, and further measurements at lower energies are required to examine the Ramsauer-Townsend region in more detail.

The positronium formation cross section is presented in Figure 3, along with two previous experimental measurements and two theoretical calculations. While all experiments agree at energies

close to the threshold, there is a divergence between the two previous measurements above about 30 eV scattering energy. The present measurements are in better agreement with the data of Marler et al. [22], although given the present error, it is difficult to make a definitive statement in this regard. The two calculations disagree with all experiments in the near threshold region and, at higher energies the calculation of McAlinden and Walters [23] is favoured by the present experimental results over the calculations of Gilmore [24]. The agreement between the measurements of Marler et al. and the present results suggest that speculation of systematic errors in the data of Laricchia et al. [25] may be correct. There has been disagreement between the two experimental groups for Ps formation cross sections for positron scattering from all the noble gases, and systematic studies to compare with all previous measurements may shed further light on this matter. It is clear that theoretical descriptions of this problem need to be improved to match the observations, and it may be that this will also provide an avenue by which to resolve the present disagreements.

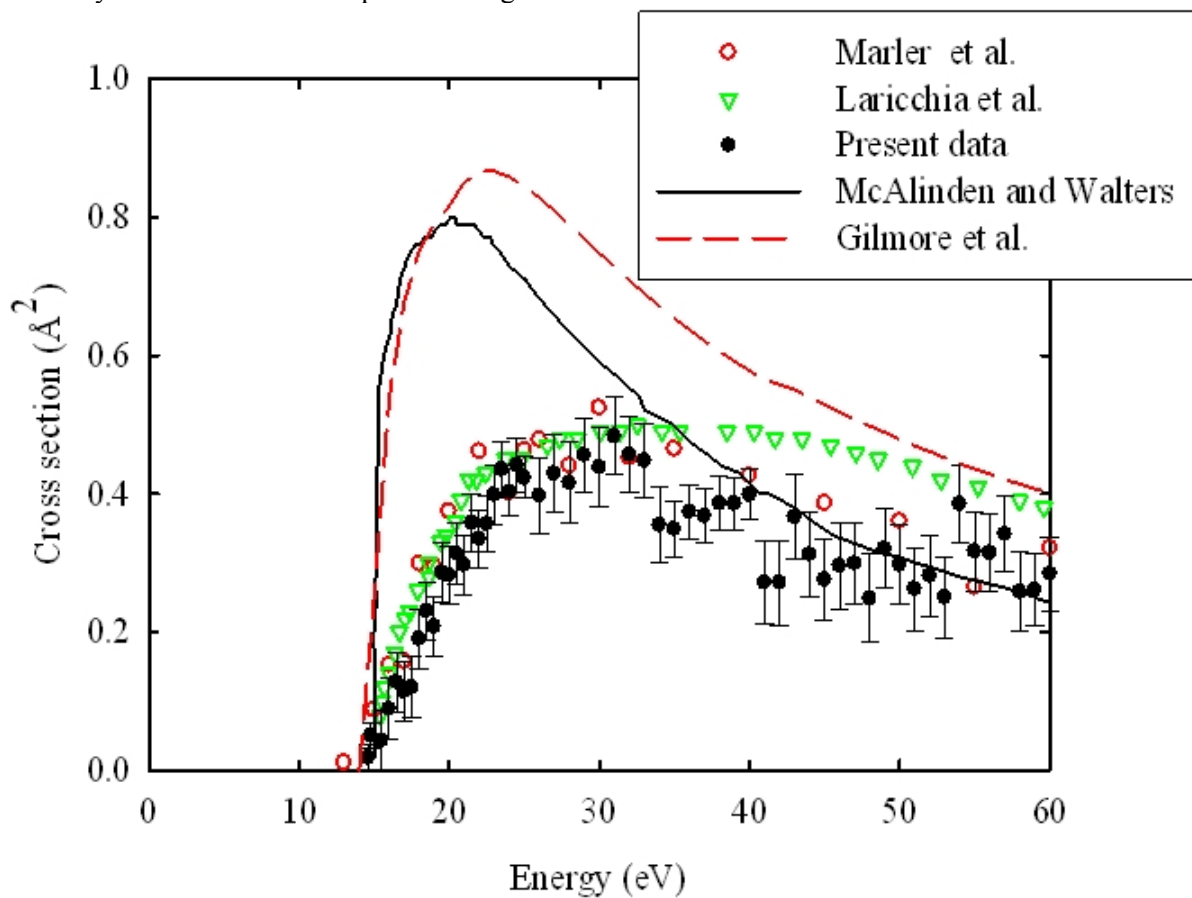


Figure 3: Positronium formation cross section for neon. The present data is compared to the previous measurements of Marler et al [22] and Laricchia et al [25] and the calculations of McAlinden and Walters [23] and Gilmore et al. [24]

### 3. Positron transport and thermalization

#### 3.1. Input data

The intrinsic property of charged particle swarm calculations is that they HAVE to include complete processes responsible for number changing, momentum transfer and energy transfer collisions. Complete does not mean every little detail but that global balance should be made regardless of how the partial contributions are distributed among the processes. This may lead to non-uniqueness which may only be resolved by the input of additional data, either transport coefficients or groups of cross

sections from other sources that are assumed to be accurate. But most importantly, the cross section sets used in (or obtained from) the swarm analysis MUST have a complete set of cross sections in the relevant energy range and until recently such data were not available. Recently, with the extended use of the Surko trap and other techniques (Recent advances in experimental techniques have enabled measurements of a wide range of inelastic cross sections for positron scattering on atoms and molecules [26, 27, 28, 29].) it became possible to make reasonably complete sets in the region of energies below the threshold for ionization and while there were no experimental transport data to compare to it was worth performing calculations to see what kind of phenomena may be found in positron transport.

In this paper we will mainly show the data for positrons in argon (as described in paper by Šuvakov et al [30]) and to make a complete set we have used

- a) The elastic momentum-transfer cross section (MTCS) and isotropic scattering of McEachran [31] as this calculation is in reasonable agreement with the existing experimental data for total cross sections [32, 33].
- b) Experimental results for the electronic excitation of the two lowest lying 3p4s J = 1 levels of argon and theoretical results were used to form effective cross sections [34, 35].
- c) Excitation of higher singlet levels based on that for electron impact excitation of argon [36].
- d) The positronium (Ps) formation and ionization cross sections were taken from the work of Marler et al [22]. These results are in good quantitative agreement with an alternative approach of Laricchia et al [25]. It is important to note that Ps formation cross section is typically two orders of magnitude larger than the equivalent process for losses of electrons, the electron attachment. And while Ps formation is a non-conservative (number changing) process for positrons, the ionization is not which is different from electron transport.
- e) Direct annihilation has been neglected as the cross section is known to be several orders of magnitude lower than that for Ps formation [37].

With this set it is reasonable to assume that we may have a very good qualitative and a reasonable quantitative prediction of the positron transport for energies up to 20 eV.

### 3.2. Basic definitions of transport coefficients

In modelling of the transport of charged particles the connection between experiment and theory is usually made through the equation of continuity

$$\frac{\partial n(\mathbf{r}, t)}{\partial t} + \nabla \cdot \mathbf{\Gamma}(\mathbf{r}, t) = S(\mathbf{r}, t), \quad (1)$$

where  $n(\mathbf{r}, t)$  is the number density of swarm particles (positrons), while  $\mathbf{\Gamma}(\mathbf{r}, t) = n\langle \mathbf{v} \rangle$  is the swarm particle flux and  $S(\mathbf{r}, t)$  represents the production rate per unit volume per unit time arising from non-conservative collisional processes such as Ps formation or annihilation. It is important to note that the average/drift velocity of the swarm is usually several orders of magnitude smaller than the instantaneous random velocities of the particles.

Far from boundaries, sources and sinks, the hydrodynamic regime is assumed to apply. In this regime, the space-time dependence of the quantities is expressible in terms of linear functionals of  $n(\mathbf{r}, t)$ , generally a density gradient expansion. Assuming this functional relationship, the flux  $\mathbf{\Gamma}(\mathbf{r}, t)$  and source term  $S(\mathbf{r}, t)$  in the continuity equation are expanded as:

$$\mathbf{\Gamma}(\mathbf{r}, t) = \mathbf{W}_F n(\mathbf{r}, t) - \mathbf{D}_F \cdot \nabla n(\mathbf{r}, t) \quad (\text{Fick's law}) \quad (2)$$

$$S(\mathbf{r}, t) = S^{(0)} n(\mathbf{r}, t) - \mathbf{S}^{(1)} \cdot \nabla n(\mathbf{r}, t) + \mathbf{S}^{(2)} : \nabla \nabla n(\mathbf{r}, t) \quad (3)$$

where  $\mathbf{W}_F$  and  $\mathbf{D}_F$  define respectively the *flux* drift velocity and *flux* diffusion tensor. Substitution of expansion the expressions for the source and flux into the continuity equation yields the diffusion equation,

$$\frac{\partial n}{\partial t} + \mathbf{W}_B \cdot \nabla n - \mathbf{D}_B : \nabla \nabla n = -R_a n, \quad (4)$$

where

$$R_a = -S^{(0)} \quad (\text{loss rate}), \quad (5)$$

$$\mathbf{W}_B = \mathbf{W}_F + \mathbf{S}^{(1)} \quad (\text{bulk drift velocity}), \quad (6)$$

$$\mathbf{D}_B = \mathbf{D}_F + \mathbf{S}^{(2)} \quad (\text{bulk diffusion tensor}). \quad (7)$$

In swarm experiments it is generally the bulk transport coefficients which are measured and tabulated. The reader is referred to Robson et al. [38] for a detailed discussion on the types and application of these transport coefficients. Physically, the bulk transport coefficients are associated with the swarm's centre of mass transport (and spread about its centre of mass) while the flux quantities are essentially averages in velocity space. The explicit influence of non-conservative collisional processes (such as Ps formation) on the swarm's centre of mass transport is described by the terms  $\mathbf{S}^{(1)}$  and  $\mathbf{S}^{(2)}$ . Obviously, in the absence of non-conservative processes, the two sets of transport coefficients coincide. The differences between, and implications associated with, the two sets of transport coefficients will be highlighted later and the differences associated with Ps formation can be particularly large.

### 3.3. Calculations of transport properties

Two independent techniques for calculation of positron transport in gases under non-equilibrium conditions are the Monte-Carlo simulation and the Boltzmann equation solution. Details of the two techniques have been reviewed elsewhere, and here we give a brief overview of each of the two techniques.

#### 3.3.1. Monte-Carlo simulation:

The Monte Carlo simulation technique for purely electric field and for the orthogonal configuration of electric and magnetic fields has been discussed in our previous papers [39, 40].

The actual code used in this calculation has been described briefly in [41, 30] as is based on similar principles as our previous work. It has been tested to satisfy all the benchmarks as our previous code and to give even better results than before that only limited by the statistical uncertainty.

We employ the coordinate system where the electric field  $\mathbf{E}$  defines the z-axis, while the magnetic field  $\mathbf{B}$  lies in the y-z plane, making an angle  $\psi$  with respect to the electric field  $\mathbf{E}$ . Hence, the equations of electron motion can be given analytically and the reader is referred to [42] for an explicit form of these equations.

The only unknown in the MC procedure is the time step for the determination of the exact moment of the next collision. This is determined by solving the equation for the collision probability, using either the null-collision [43] or integration technique [44]. In our code, the latter approach is employed. All dynamic properties of each electron such as the position, velocity and energy can be updated and the electron motion through the neutral gas can be followed between collisions.

The angular distributions of both elastic and inelastic collisions are taken to be isotropic. It must be emphasized that this approximation is generally valid for relatively low E/N but needs to be corrected when forward scattering becomes dominant. In that respect, Biagi has adopted the method proposed by Longo and Capitelli [45] in his Monte Carlo code to include the angular distribution of both elastic and inelastic collisions [42]. For CF<sub>4</sub>, it was shown by Vasenkov [46], the errors in transport coefficients, resulting from the assumption of isotropic scattering are less than about 3% for E/N below 0.1 Td. For higher E/N, the errors increase rapidly up to 35%. In addition, it is necessary to reconsider the influence of superelastic collisions in an effort to account properly for the behavior of electron swarms at low energies. However, since we attempt to scan a wide range of transport coefficients and to provide a database for plasma modeling, we will not focus on these issues in the present paper.

### 3.3.2. Transport coefficients, definitions and calculations

Transport coefficients up to diffusion are determined after relaxation to the steady state from the formulae described in [47, 48, 49]. The number changing reaction rate is defined by

$$\alpha = -\frac{d}{dt}(\ln N), \quad (8)$$

the bulk drift velocity by

$$\mathbf{W}_B = \frac{d}{dt}\langle \mathbf{r} \rangle, \quad (9)$$

and the bulk diffusion tensor by

$$\mathbf{D}_B = \frac{1}{2!} \frac{d}{dt} \langle \mathbf{r}^* \mathbf{r}^* \rangle. \quad (10)$$

where  $\mathbf{r}^* = \mathbf{r} - \langle \mathbf{r} \rangle$ . These are the so-called ‘‘bulk’’ transport coefficients that are established from the mean position of the electron swarm in the configuration space [50].

In the absence of the non-conservative collisions, one may avoid the differentiation required to obtain the drift velocity and components of the diffusion tensor by using the so-called ‘‘flux’’ quantities. Hence the flux drift velocity and the flux diagonal elements of the diffusion tensor are given by:

$$W_{F,i} = \left\langle \frac{dx_i}{dt} \right\rangle = \langle v_i \rangle, \quad (i = x, y, z), \quad (11)$$

$$D_{F,xx} = \langle xv_x \rangle - \langle x \rangle \langle v_x \rangle, \quad (12)$$

$$D_{F,yy} = \langle yv_y \rangle - \langle y \rangle \langle v_y \rangle, \quad (13)$$

$$D_{F,zz} = \langle zv_z \rangle - \langle z \rangle \langle v_z \rangle. \quad (14)$$

It follows from (9) that bulk drift velocity is displacement of the mean position of the electron swarm and it describes the motion of the centre of mass of the total ensemble of electrons. On the other hand, the flux drift velocity is the mean velocity of electrons. These two sets of transport coefficients are equal by definition, as mentioned above, in the absence of non-conservative collisions (ionization/attachment), however in the presence of non-conservative processes they may differ. The distinction between these two sets of transport coefficients was discussed at length in the 1980’s (see [50]), but has been ignored in the majority of previous work in plasma modeling community. This has lead to a potentially serious mismatch between input swarm data (generally the bulk transport properties) and the parameters (often the flux transport properties) required in many plasma fluid models [51,52]. Note that only theory, i.e., Boltzmann equation calculations and/or Monte Carlo simulations, can resolve any such mismatch, by providing both flux and bulk transport coefficients.

Typically we follow 10 000 to 1000 000 particles through a large number of collisions. In all cases our results were in excellent agreement with those obtained by numerical solution to the Boltzmann equation.

### 3.3.3. Boltzmann equation solution:

The starting point of any kinetic theory calculation is the Boltzmann equation, which can be written in generic form as

$$\left[ \frac{\partial}{\partial t} + \mathbf{v} \cdot \nabla + \frac{e}{m} (\mathbf{E} + \mathbf{v} \times \mathbf{B}) \cdot \frac{\partial}{\partial \mathbf{v}} \right] f = J(f) \quad (15)$$

This is essentially a continuity equation for  $f$  in phase-space. For swarms, only one species of charged particle is usually present in the gas,  $\mathbf{E}$  and  $\mathbf{B}$  are prescribed external fields, and the electron-



electron (or ion-ion) mutual interaction term is neglected in the collision operator  $J(f)$ . The kinetic equation is thus linear in  $f$ .

Solution of the Boltzmann equation is generally made through representations of the space and velocity dependence of  $f(\mathbf{r}, \mathbf{v}, t)$ . Under hydrodynamic conditions the space-time dependence of  $f(\mathbf{r}, \mathbf{v}, t)$  is represented in the form of a density gradient expansion (detailed above). The velocity dependence in  $f(\mathbf{r}, \mathbf{v}, t)$  is generally represented in terms of a combined spherical harmonic and modified Laguerre basis set (combined generally referred to as Burnett functions). This set is complete on velocity space. It is important to emphasize that this is a true multi-term technique (i.e. as many spherical harmonics are retained as required to achieve the accuracy criterion), thus removing the restrictions to near isotropy in velocity space generally associated with previous positron transport studies which are based on the two-term solution of Boltzmann equation. No assumptions are made on the anisotropy of the differential cross-sections. Matrix elements of the Boltzmann equation are then made, and a hierarchy of coupled matrix equations is formed for the moments of the distribution function. The transport properties and coefficients detailed above can then be represented in terms of these moments. For further details the reader is referred to the reviews of Robson and Ness [53] and White et al. [54].

#### 4. Thermalization of positrons in $N_2$

In Monte Carlo simulations the particles have to start from some initial distribution. While proper swarm experiments require that the temporal relaxation be complete and spatial relaxation extends over a small portion of the gap between the two electrodes, the simulation follows the development of the swarm from the initial or boundary conditions and we may then choose to follow the space/time development of the properties or to wait until relaxation is complete to start sampling. Thus we may use the same tool to model thermalization experiments, low energy transport coefficients and also, to perhaps model some applications.

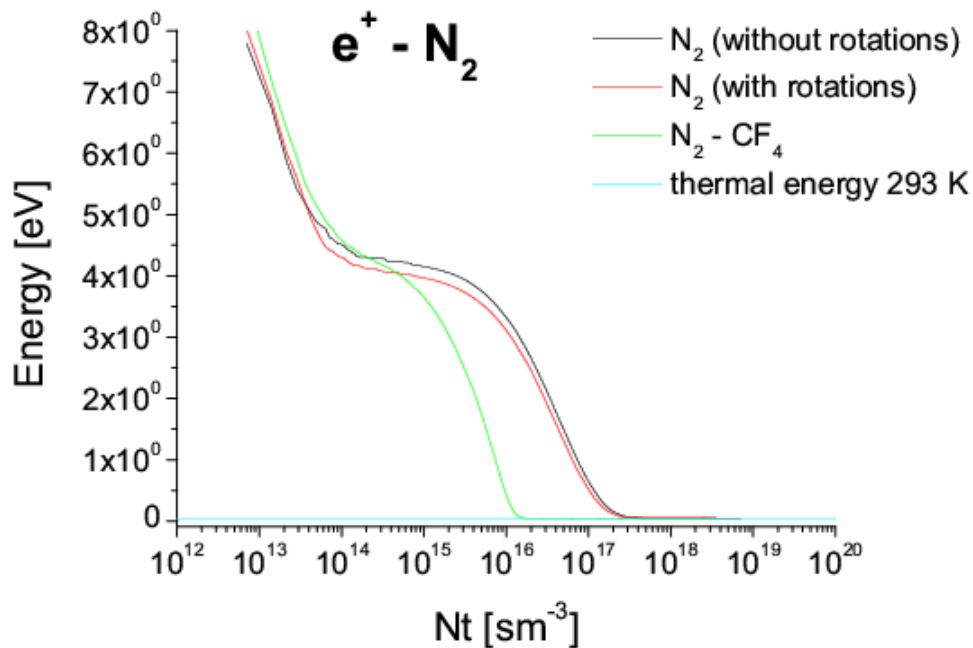


Figure 4. Thermalization of the mean energy of positrons from a Maxwellian initial distribution with a mean starting energy of 10eV in  $N_2$  and  $N_2$ - $CF_4$  mixture

One example of the calculation of temporal relaxation to the thermal energy which is equivalent to modelling of a thermalization experiment is given for the case of nitrogen: In Figure 4 we show the temporal development of the mean energy of an ensemble of positrons in nitrogen (for the cross sections and other information check [55]). It is possible to isolate a time/energy region where different processes dominate the thermalization.

We have also compared the calculated values of thermalization times in different gases (see Table 1) and obtained a good agreement with the measurements of Charlton and his colleagues [56].

gas	Nt (sm <sup>-3</sup> ) Present results	Nt (sm <sup>-3</sup> ) Al-Qaradawi et al (2000)
N <sub>2</sub>	2.5*10 <sup>17</sup>	3.8*10 <sup>17</sup>
N <sub>2</sub> -CF <sub>4</sub>	1.4*10 <sup>16</sup>	X
H <sub>2</sub>	4.5*10 <sup>16</sup>	6.5*10 <sup>16</sup>

Table. Comparison between the thermalization times calculated using our Monte Carlo code and measured by Al-Qaradawi et al. [56].

Spatial relaxation was followed by simulations starting from a point with mono-energetic distribution function and allowing the swarm to spread in the electric field in hydrogen gas [57]. While one could expect that Ps formation could erase the oscillatory variation of the averaged properties we see that it is neither the case for the momentum nor for the energy relaxation.

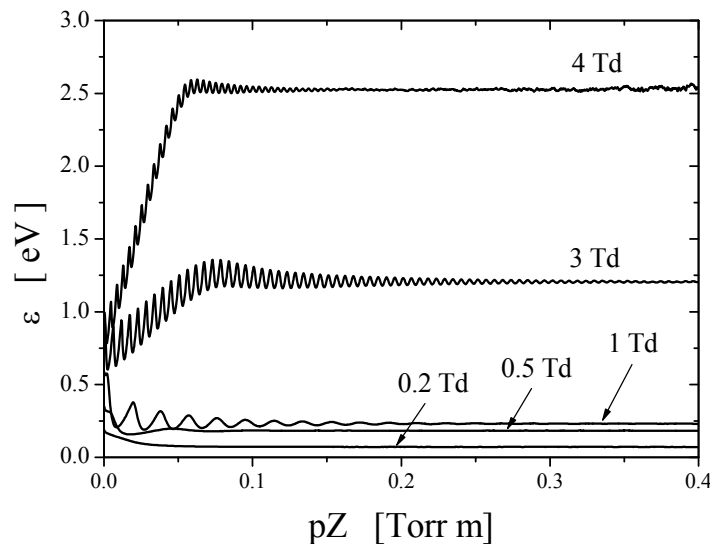


Figure 5. Spatial relaxation of the mean energy for positrons in hydrogen for different E/N as indicated in the graph [57].

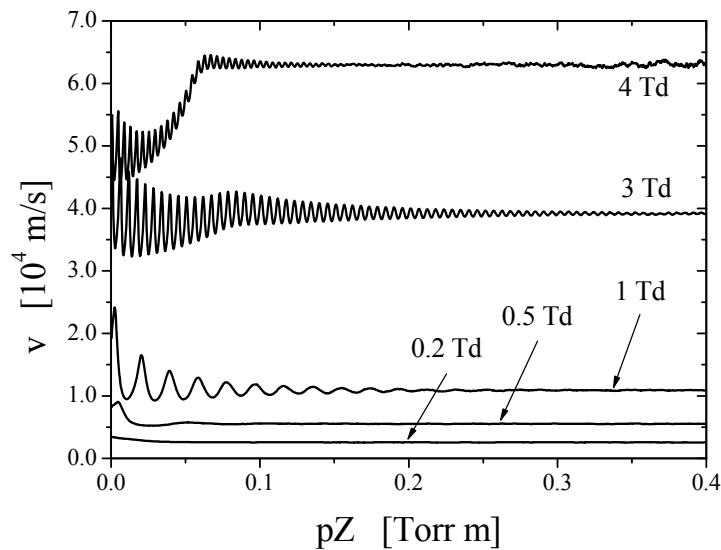


Figure 6. Spatial relaxation of the average velocity for positrons in hydrogen for different E/N as indicated in the graph [57].

Since all these calculations were made for the temporal and spatial development in a gas and the results are scaled either through  $Nt$  or  $Nd$  (or  $pZ$ ), the results are relevant and directly applicable for gas phase relaxation in gas under conditions even equivalent to the collisional traps. These results however, are, as can be seen from comparisons above, directly applicable for gas thermalization measurements.

### 5. Non-equilibrium transport: Positron transport in Ar

Recently, there has been a renewed interest in the calculation of non-equilibrium transport properties of positron swarms in gases under the influence of electric fields [55, 58, 30]. There has been a host of striking phenomena, including the existence of negative differential conductivity (NDC) only for the bulk drift velocity in both atomic and molecular gases.

Of particular note is the magnitude of the Ps formation cross-section with a threshold of around 7eV for the case of Ar. The magnitude of the Ps formation cross-section is greater than both the elastic and excitation cross-sections over an extended energy range to approximately 30eV. As detailed in Šuvakov et al. [30], the Ps formation cross-section has a dramatic impact on the transport properties of the positron swarm due to the explicit non-conservative action of the Ps formation on the transport properties. The initial calculations for positrons in Ar were made using the Monte-Carlo simulation technique developed by the Petrović's group and the set of cross-sections detailed above. The neutral temperature is assumed to be 0K in these calculations. All scattering is assumed to be isotropic. In what follows, we present a comparison of the Boltzmann equation solution results with the MC simulation results [30] for positrons in Ar.

In Figure 7 and Figure 8, we display the mean energy and drift velocities (bulk and flux) of the swarm as a function of E/N (where N is the gas number density). Over the range of E/N we observe very good agreement between the two independent techniques for both the mean energy and the flux drift velocity. Convergence problems with the Boltzmann equation calculation of the bulk drift velocity in the vicinity of 10 Td were experienced, however the general behavior detailed in Šuvakov et al. [30] in this region are clearly reinforced.

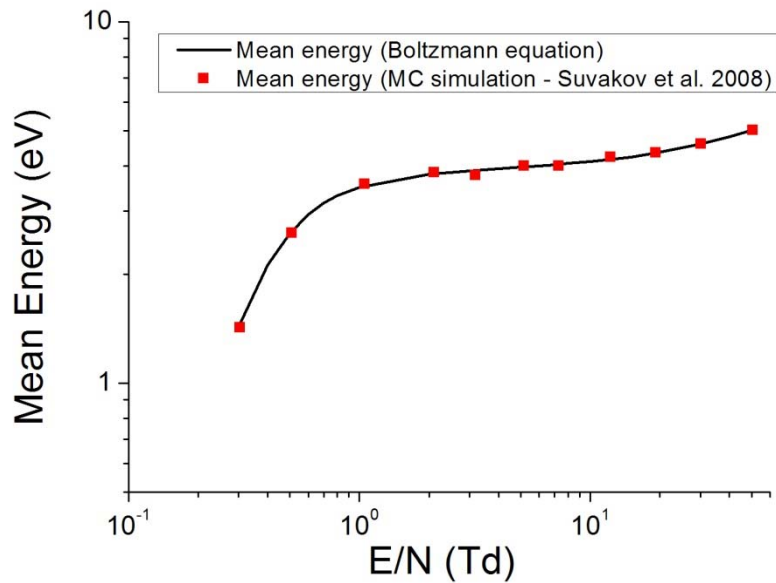


Figure 7: Comparison of the Boltzmann equation solution with the MC simulation results of Šuvakov et al. [30] for the mean energy of positron swarms in Ar as a function of E/N.

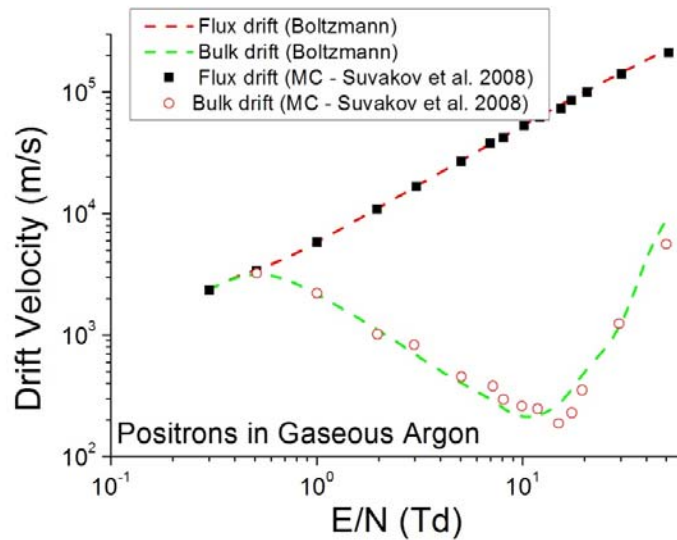


Figure 8: Comparison of the Boltzmann equation solution and the MC simulations of Šuvakov et al. [30] for the bulk and flux drift velocities of positron swarms in Ar as a function of E/N.

The striking phenomenon of NDC in the bulk drift velocity is clearly evidenced in Figure 8. The flux drift velocity does not exhibit such behavior. The NDC in the bulk drift velocity is explicitly due to the influence of Ps formation on the centre-of-mass of the positron swarm. Over the region of E/N considered, the Ps formation processes are preferentially taking positrons from the higher energy part of the energy distribution. Since positrons at the front of the swarm have generally fallen through a

greater potential, they are generally higher in energy. Thus, Ps formation is preferentially taking positrons from the front of the swarm and consequently the modification to the centre of mass motion brought about by this process acts to decrease the bulk drift velocity relative to the flux drift velocity. Of course, there is an implicit effect associated with the cooling effect on the positron swarm due to the preferential loss of higher energy positrons (reducing the mean energy over what it would have been).

The effect of NDC is inherently different from that for electrons as it is solely induced by the non-conservative nature of the Ps formation. This was shown by the calculations shown in [30] where Ps formation was treated as a conservative inelastic process. While a small change in the mean energy followed from this change in the nature of the collisions both flux and bulk drift velocities were identical and very close to the flux drift velocity in the case of transport for realistic Ps formation. The possibility of NDC induced by a non-conservative process was first predicted by Vrhovac and Petrović [59] but based on the experience with the electrons it was predicted that bulk NDC was possible only if the conditions are also met for the flux, i.e. so that either NDC or at least a plateau exist for the flux drift velocity. In this case the flux drift velocity does not show any sign of NDC while the bulk property drops by two orders of magnitude.

The relationship between the flux and bulk drift velocity may be calculated if one takes into account the rate of the non-conservative process (in this case  $v_{PF}$  the Ps formation rate). It was found [50] that the bulk drift velocity may be estimated to first order from the flux value as follows:

$$W_B = W_F - \frac{2\varepsilon}{3e} \frac{dv_{PF}}{dE} \tag{16}$$

where  $\varepsilon$  is the mean energy,  $E$  the electric field and in the case of particle loss the bulk property is smaller than the flux drift velocity. In Figure 9 we show how such calculation would work for positrons in argon [60].

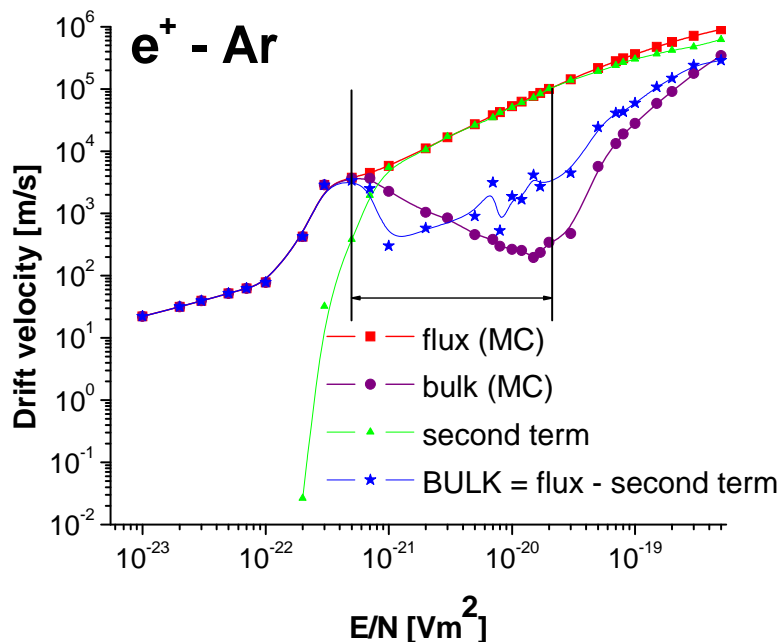


Figure 9. The calculation of the bulk drift velocity (stars) determined from the MC flux drift velocity (squares) by subtracting the second term in equation (16). The results are compared to the results of direct MC simulation (circles) [60]

The calculated bulk drift velocity agrees qualitatively with the result of direct simulation but quantitatively there are some discrepancies mainly due to very close values of the two terms that are subtracted. A much better agreement between simulations and the application of the formula was achieved for N<sub>2</sub> [60]. It was proposed that due to a very large degree of skewing of the spatial distribution of the swarm of particles the simple, first order formula (16) may not be sufficiently accurate and more exact treatment may be required but nevertheless it provides a physical explanation of the process.

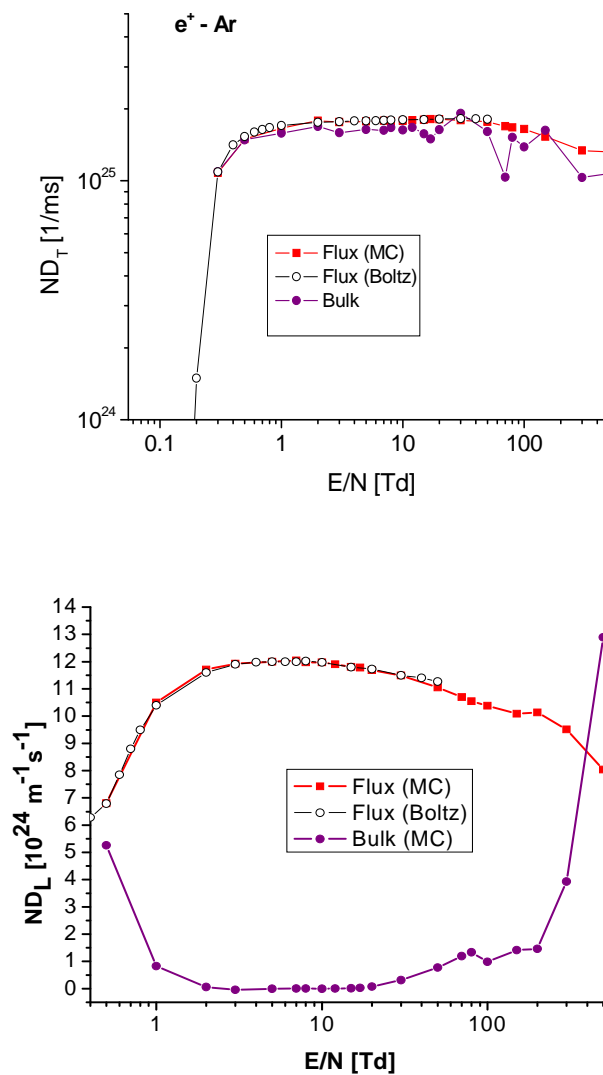


Figure 10. The results of simulations (MC) for (a) transverse and (b) longitudinal components of the diffusion tensor [30]. Results are compared with the Boltzmann equation (Boltz) results where available.

Šuvakov et al. [30] found that in an almost similar fashion the bulk diffusion coefficient in the longitudinal direction is affected by the positronium formation, while this has not been observed either for the transverse diffusion or for both flux diffusion coefficients. The results of simulation for the diffusion coefficients are shown in Figure 10. The diffusion coefficients are more difficult to obtain

due to the need to sample more complex quantities and the subsequent differentiation needed to produce bulk properties may lead to somewhat more scattered results. Yet we may conclude that for all practical purposes transverse diffusion coefficients are identical, while the two order of magnitude differences observed in the longitudinal components can certainly not be explained by statistical uncertainty. The almost zero value of the diffusion coefficient along the direction of electric field occurs in a similar E/N region as the NDC yet it has a different shape and value. As could be expected this feature disappears as the Ps formation changes its magnitude.

## 6. Conclusion

High resolution measurements of positron scattering from neon have been compared to previous experimental and theoretical work. While the experiments have a much better resolution than previous work (with the exception of the data of Marler et al. [22]) and a high statistical accuracy, there remain unresolved discrepancies in the grand total cross section determination. In the case of the positronium formation cross section, present results favor the measurement of Marler et al., but higher statistical accuracy is required before any definitive conclusions can be made. Future work in this regard will concentrate on better quality measurements of the positronium formation cross section, as well as high resolution measurements of cross sections at both low energy (in the case of the total cross section) and around threshold regions for positronium formation, electronic excitation and ionisation. It is anticipated that a program of inelastic scattering measurements will be undertaken in the future, as well as measurements of differential scattering cross sections.

In the swarm part of the activity of our collaboration it was found that with the newly measured and calculated data reasonably complete sets of cross section data may be found. These sets provide a very good qualitative picture of the transport of swarms and predict a new set of kinetic phenomena that could not be observed for electrons because of the large difference in the magnitude of the non-conservative cross sections for the two types of particles. The most important effect is that of the NDC for the bulk drift velocity even when there is no indication of NDC for the flux drift velocity. Additional tests show that the effect is ONLY induced by the non-conservative nature of the Ps formation and it is not the result of the shape of the cross sections. This effect together with almost zero diffusion in the longitudinal direction and with a very large degree of skewness of the spatial time of flight are worthy of further investigation. For these reasons alone it would be worthwhile to reopen the positron swarm experiments which have had a large degree of difficulty in the past and presently exist only in measurements of thermalization times [8]. On the other hand with more accurate measurements of swarm parameters it would be possible to test the sets of cross sections and in particular, based on accurate measurements of some processes, renormalize the contribution of the missing processes. While Monte Carlo codes, as presented here, still have a long way to go to be applicable in modelling of applications in liquids and living tissues they are based on best available cross section data rather than semi-empirical formulae and therefore should be a better representation of the physics in a broader set of circumstances. Presently tests of codes are based on comparisons of calculated trajectories which is not sufficient. A more rigorous test, as 50 years of swarm physics teach us, would be to compare accurate values of well defined averaged transport coefficients especially if those could be collaborated by measurements from experiments.

## Acknowledgements

The work presented here was supported by MNTRS grant 141025. The authors are grateful to the Australian Research Council for support under the Centers of Excellence Program and to the Australian Government Department of Innovation, Industry, Science and Research for support under the International Linkages Program. In particular we are grateful to our colleagues M. Charlton, R. Robson and C. Surko on useful comments and discussions on the topics related to this work.

## References

- [1] Brunger MJ and Buckman SJ 2002 *Phys. Reports* **357** 215
- [2] Buckman SJ and Clark CW 1994 *Rev. Mod. Phys.* **66** 539
- [3] Huxley LG and Crompton RW 1974 *The drift and diffusion of electrons in gases* (Wiley Interscience New York)
- [4] Crompton RW 1994 *Advances in Atomic Molecular and Optical Phys.* **32** 97
- [5] Petrović ZLj, Šuvakov M, Nikitović Ž, Dujko S, Šašić O, Jovanović J, Malović G and Stojanović V 2007 *Plasma Sources Sci. Technol.* **16** S1–S12
- [6] Christophorou LG, Olthoff JK and Rao MVVS 1996 *J. Phys. Chem. Rev. Data* **25** 1341
- [7] Makabe T and Petrović ZLj 2006 *Plasma Electronics* (Taylor and Francis, New York)
- [8] Charlton M *the present issue*
- [9] Charlton M and Humberston JW 2001 *Positron Physics* (Cambridge University Press).
- [10] Murphy T and Surko CM 1992 *Phys. Rev. A* **46** 5696
- [11] Gilbert SJ, Kurz C, Greaves RG and Surko CM 1997 *Appl. Phys. Lett.* **70** 1944
- [12] Sullivan JP, Gilbert SJ, Marler JP, Greaves RG, Buckman SJ and Surko CM 2002 *Phys. Rev. A* **66** 042708
- [13] Sullivan JP, Gilbert SJ, and Surko CM 2001 *Phys. Rev. Lett* **86** 1494
- [14] Sullivan JP, Jones A, Caradonna P, Makochekanwa C and Buckman SJ 2008 *Rev. Sci. Instr.* **79** 113105
- [15] Coleman PG, McNutt JD, Diana LM, Burciaga JR 1979 *Phys. Rev. A* **20** 145
- [16] Stein TS and Kauppila WE 1982 *Adv. At. Mol. Phys.* **18** 53
- [17] Kauppila WE, Stein TS, Smart JH, Dababneh MS, Ho YK, Downing JP, Pol V 1981 *Phys. Rev. A* **24**, 725
- [18] Tsai JS, Lebow L, Paul DAL 1976 *Can. J. Phys.* **54** 1741
- [19] Coleman PG, Griffith TC, Heyland GR and Twomey TR 1976 *Appl. Phys.* **11** 321
- [20] McEachran RP 2008 *private communication*
- [21] Baluja KL, Jain A, Jones HW, Weatherford CA, Karim KR 1991 *J. Phys. B* **24** L93
- [22] Marler JP, Sullivan JP and Surko CM 2005 *Phys. Rev. A* **71** 022701
- [23] McAlinden MT and Walters HRJ 1992 *Hyperfine Interactions* **73** 65
- [24] Gilmore S, Blackwood JE and Walters HRJ 2004 *Nucl. Instr. Meth. B* **221** 129
- [25] Laricchia G, Van Reeth P, Szluinska M and Moxom J 2002 *J. Phys B.* **35** 2525
- [26] Marler JP and Surko CM 2005 *Phys. Rev. A* **72** 062702
- [27] Marler JP and Surko CM 2005 *Phys. Rev. A* **72** 062713
- [28] Charlton M 1985 *Rep. Prog. Phys.* **48** 737
- [29] Karwasz GP 2005 *Eur. Phys. J. D* **35** 267
- [30] Šuvakov M, Petrović ZLj, Marler JP, Buckman SJ, Robson RE and Malović G 2008 *New J. Phys.* **10** No 5 053034
- [31] McEachran RP 2006 *private communication*
- [32] Karwasz GP, Pliszka D and Brusa RS 2006 *Nucl. Instrum. Methods B* **247** 68
- [33] Kauppila WE and Stein TS 1990 *Adv. At. Mol. Opt. Phys.* **26** 1
- [34] Sullivan JP, Marler JP, Gilbert SJ, Buckman SJ and Surko CM 2001 *Phys. Rev. Lett.* **87** 073201
- [35] Parcell LA, McEachran RP and Stauffer A 2000 *Nucl. Instrum. Methods B* **171** 113
- [36] Phelps AV and Tachibana K 1985 *private communication*
- [37] Barnes LD 2005 PhD Thesis University of California, San Diego
- [38] Robson RE, White RD and Petrović ZLj 2005 *Rev. Mod. Phys.* **77** 1303
- [39] Dujko S, Raspopović ZM and Petrović ZLj 2005 *J. Phys. D: Appl. Phys.* **38** 2952
- [40] Raspopović ZM, Sakadžić S, Bzenić SA and Petrović ZLj 1999 *IEEE Trans. Plasma Sci.* **27** 1241
- [41] Šuvakov M, Ristivojević Z, Petrović ZLj, Dujko S, Raspopović ZM, Dyatko NA and Napartovich AP 2005 *IEEE Trans. Plasma Sci.* **33** 532



- [42] Biagi SF 1999 *Nucl. Instrum. Methods A* **421** 234
- [43] Skullerud HR 1968 *J. Phys. D: Appl. Phys.* **1** 1567
- [44] Itoh H and Musha T 1960 *J. Phys. Soc. Japan* **15** 1675
- [45] Longo S and Capitelli M 1993 *Plasma Chem. Plasma Process.* **14** 1
- [46] Vasenkov AV 2000 *J. Appl. Phys.* **88** 626
- [47] Nolan AM, Brennan MJ, Ness KF and Wedding AB 1997 *J. Phys. D* **30** 2865
- [48] White RD, Brennan MJ and Ness KF 1997 *J. Phys. D* **30** 810
- [49] Raspopović ZM, Sakadžić S, Petrović ZLj and Makabe T 2000 *J. Phys. D: Appl. Phys.* **33** 1298
- [50] Robson RE 1991 *Aust. J. Phys.* **50** 577
- [51] White RD, Robson RE and Ness KF 1999 *Phys. Rev E* **60** 7457
- [52] Robson RE 1986 *J. Chem. Phys.* **85** 4486
- [53] Robson RE and Ness KF 1986 *Phys. Rev. A* **33** 2068
- [54] White RD, Ness KF and Robson RE 2002 *Appl Surf. Sci.* **192** 26
- [55] Banković A, Marler JP, Šuvakov M, Malović G and Petrović ZLj 2008 *Nuclear Inst. Methods, B* **266** 462
- [56] Al-Qaradawi I, Charlton M, Borozan I and Whitehead R. 2000 *J. Phys. B: At. Mol. Opt. Phys.* **33** 2725
- [57] Banković A, Dujko S, White RD, Marler JP, Malović G and Petrović ZLj unpublished
- [58] Marler JP, Petrović ZLj, Banković A, Dujko S, Šuvakov M, Malović G and Buckman SJ 2009 *Phys. Plasmas* submitted
- [59] Vrhovac SB and Petrović ZLj 1996 *Phys. Rev. E* **53** 4012
- [60] Banković A, Petrović ZLj, Robson RE, Marler JP, Dujko S and Malović G 2008 *Nucl. Instrum. Methods B* accepted doi: 10.1016/j.nimb.2008.10.034